NANO LETTERS

2008
Vol. 8, No. 8
2166-2170

FIB/TEM Characterization of the Composition and Structure of Core/Shell Cu−Ni Nanowires

Zhu Liu,[†,‡] David Elbert,[†,§] Chia-Ling Chien,[‡,⊥] and Peter C. Searson*[,‡,⊥]

Department of Materials Science and Engineering, Department of Earth and Planetary Sciences, and Department of Physics and Astronomy, Johns Hopkins University, Maryland 21218

Received February 19, 2008; Revised Manuscript Received May 19, 2008

ABSTRACT

Characterization of composition and structure is crucial to understanding the properties and performance of nanomaterials. For nanowires and nanotubes, determining radial compositional and structural modulations is particularly challenging. Here we use a focused ion beam (FIB) lift-out technique to show that Cu−Ni core/shell nanowires fabricated by template synthesis are characterized by large, high purity (>99 atom %) copper grains surrounded by much smaller, high purity (>99 atom %) nickel grains.

Nanomaterials with high aspect ratios, such as nanowires,[1–4] nanoporous nanowires,[5] and nanotubes[6–8] have potential applications in solar cells,[9,10] chemical sensors,[11] bioseparations,[12] optical barcodes,[13] and drug delivery.[12,14] The physical properties of these materials are intimately related to the composition and structure, and hence characterization using tools such as transmission electron microscopy (TEM) is crucial for materials development.

Core/shell nanowires provide a novel class of nanomaterials that are characterized by a radial variation in composition and microstructure. For example, core/shell semiconductor nanowires have been exploited in p-i-n solar cells.[15] In previous work,[16] we have demonstrated that electrodeposited Cu−Ni films form a novel microstructure characterized by nodular features with a copper-rich core and nickel-rich shell. By confining deposition to a porous template with appropriate pore dimensions, single core/shell nanowires can be produced. Chemical etching of the copper-rich phase reveals a nickel-rich tube, implying a structure with a copper-rich core and nickel-rich shell.

The focused ion beam (FIB) lift-out technique allows site-specific preparation of TEM sections from a range of sample materials.[17–19] Here, we report a new application that allows direct investigation of the radial structure of nanowires. Our combination of cross-sectional FIB and TEM provides direct evidence for phase separation that complements other techniques, such as X-ray diffraction, while revealing differences in grain size and compositional distribution between the core and shell regions.

For TEM characterization, nanowires are usually suspended in a solvent and dispersed on a grid.[1,3,15,20] This method is relatively straightforward and convenient but has two principal drawbacks. First, since imaging is performed perpendicular to the nanowire axis, the nanowires need to be less than about 50 nm in diameter to extract useful information. Second, in this geometry it is very difficult to obtain cross-sectional information. For nanowires with axial compositional or structural modulations, such as multilayered nanowires,[1] imaging perpendicular to the nanowire axis is ideal for characterization of the layer thicknesses and interface quality. For nanowires with radial structural or compositional variations, however, imaging parallel to the nanowire axis is essential.

Figure 1 shows X-ray diffraction patterns for our Cu−Ni nanowires demonstrating phase separation. Details of the template synthesis have been described elsewhere.[16] The diffraction pattern for the as-deposited nanowires shows two peaks close to the values of 2θ for Cu(111) and Ni(111), indicating the formation of a copper-rich phase and a nickel-rich phase. Copper and nickel have similar lattice parameters ($a_{Cu} = 0.3615$ nm, $a_{Ni} = 0.3524$ nm) and are generally thought to exhibit solid solubility across the whole compositional range. Recent reports, however, demonstrate a miscibility gap below 600 K.[21,22]

The Cu-rich phase can be selectively etched from the nanowires by applying a positive potential. Although copper

* To whom correspondence should be addressed. E-mail: searson@jhu.edu.
† These authors contributed equally.
‡ Department of Materials Science and Engineering, Johns Hopkins University.
§ Department of Earth and Planetary Sciences, Johns Hopkins University.
⊥ Department of Physics and Astronomy, Johns Hopkins University.

10.1021/nl080492u CCC: $40.75
Published on Web 07/16/2008

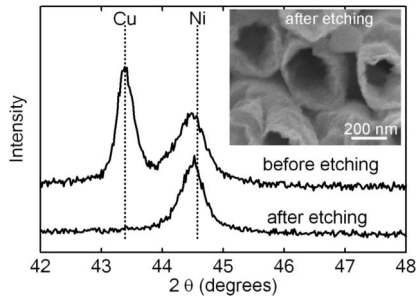

Figure 1. X-ray diffraction patterns of Cu−Ni nanowires before and after Cu etching. The nanowires were deposited at −0.9 V (Ag/AgCl) into an alumina template with a pore diameter of 220 nm from solution containing 50 mM $CuSO_4$, 400 mM $Ni(N_2HSO_3)_2$, and 0.65 M HBO_3. The Cu was selectively etched at 0.5 V (Ag/AgCl) in the same solution. The inset shows an SEM image of Cu−Ni nanowires after etching.

is more noble, nickel forms a protective passive film in sulfamate solution and hence the copper can be selectively etched.[23,24] The X-ray diffraction pattern of the nanowires after etching shows a single peak corresponding to the nickel-rich phase. The SEM image of the Cu−Ni nanowires after etching (Figure 1) reveals a tube geometry suggesting a core/shell structure.

The FIB work was done using a Ga^+ beam in a dual-beam instrument (FEI, Nova-600) with a micromanipulator working edge-on to the nanowires still in the template. Prior to FIB milling, a small piece of the alumina template containing the nanowires was coated with a thin (∼10 nm) layer of gold to reduce charging during electron- or ion-beam imaging. The sample was then mounted vertically on the sidewall of the sample stage with the template cross-section uppermost and the nanowires horizontal. The lift-out technique, detailed in Figure 2, involves cutting a 2 μm thick foil out of the template, using a micromaniulator within the FIB chamber to move the sample to a TEM grid, followed by final thinning and cleaning on the TEM grid.

Figure 2a shows part of the template viewed from above; note that the side where deposition was initiated is at the top and the nanowires are about 15 μm long. As shown in Figure 2b, prior to ion-beam milling, a 2 μm thick rectangular platinum stripe about 2 × 20 μm is deposited on the template cross-section using the FIB gas injection system (GIS). This stripe is deposited over the area of interest and protects the underlying sample from ion-beam damage during milling. The FIB is then used to mill out the template on either side of the platinum stripe (Figure 2c). This milling leaves a 2 μm thick foil standing vertically in the template. This foil is then partially cut free by milling through one side, the bottom and part of the second side (Figure 2d).

Moving the foil to the TEM grid involves affixing the micromanipulator probe by deposition of Pt using the FIB GIS (Figure 2e) and milling through the remaining contact with the bulk sample to free it from the template (Figure 2f). The sample is then positioned against the TEM grid (Figure 2g), secured with GIS deposited Pt, and cut free from the micromanipulator tip (Figure 2h). For these steps, ion milling was performed at 30 keV with beam currents of 1−5 nA. Platinum deposition utilized beam currents of 0.1−0.5 nA.

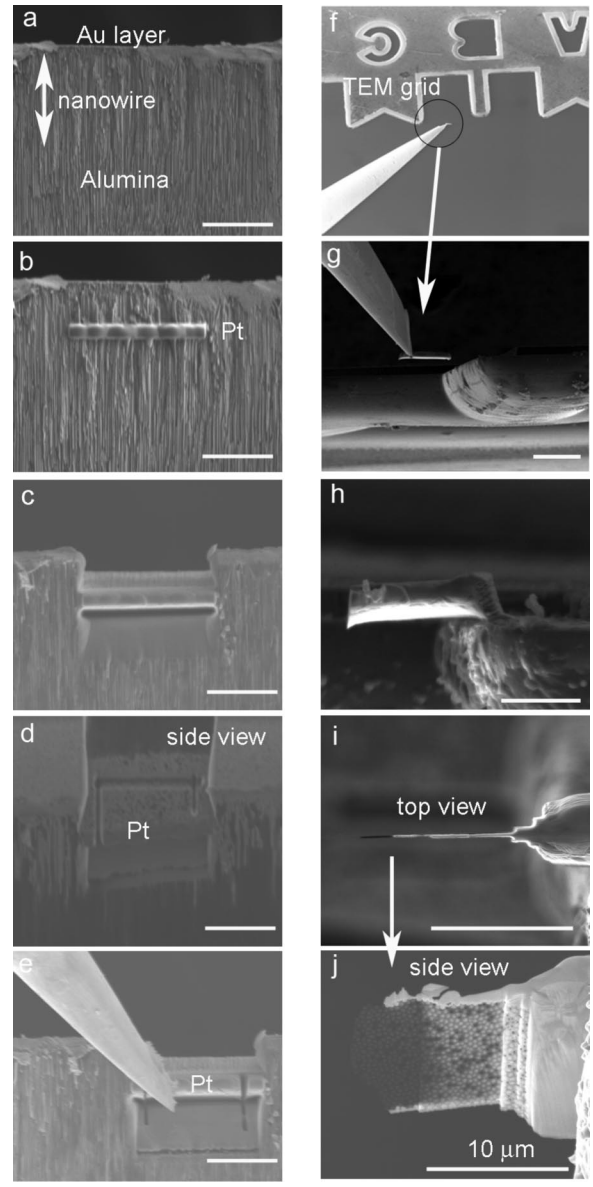

Figure 2. SEM images illustrating the steps in the FIB lift-out technique to prepare TEM cross sections. All scale bars are 10 μm. (a−f) SEM images taken in the ion beam channel; (g−j) SEM images taken in the electron beam channel. (a) The alumina template containing the nanowires is vertically mounted on the side wall of the stage with the nanowires oriented horizontally; (b) a Pt strap is deposited over the area of interest; (c) ion milling is used to mill away the sample adjacent to the Pt covered region; (d) after rotation of the stage, the sample is partially cut free from the bulk (e) the micromanipulator tip is welded to the Pt stripe; (f,g) the sample is transferred to the TEM grid; (h) the sample is attached to the TEM grid by depositing Pt then cut free from the micromanipulator; (i) side view and (j) top view of the nanowire sample after thinning.

Once secured on the TEM grid, the sample is thinned to electron transparency using ion milling nearly parallel to the large plane of the foil. To minimize sample damage, the beam current is dropped to ∼0.1 nA for the final micron of thinning and the face of the foil is never scanned with the ion beam. Final thickness was 50−90 nm. Final cleaning of the sample

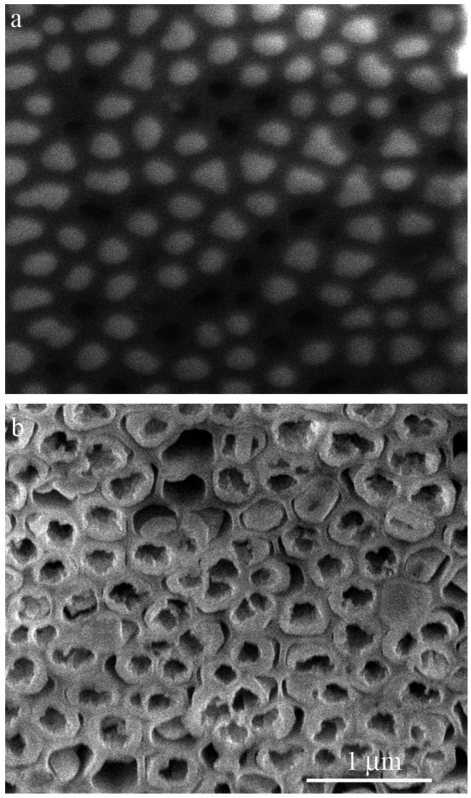

Figure 3. Cross section, secondary-electron images of Cu−Ni nanowires (light) inside the template (dark): (a) before etching and (b) after etching the copper core.

was done with a 5 kV, 70 pA beam to remove surface layers containing damage from the 30 kV thinning and ensure minimal damage in the final sample.[25]

Figure 3 shows SEM cross-section images of the Cu−Ni nanowires in the template before and after etching. The SEM images of the as-deposited Cu−Ni nanowires show that the pores are not circular, typical of the alumina templates, and that some nanowires (<15%) are missing, most likely as a result of the sample preparation process. The Cu-rich and Ni-rich phases cannot be distinguished in the SEM by imaging. Low-voltage, SEM-based EDS investigation can provide spatial resolution less than 100 nm but would require the use of Cu and Ni L-shell X-rays whose substantial peak overlap make quantitative analysis intractable.[26] After etching, the core is removed leaving the tubular shell, as described above.

Figure 4a shows bright field TEM images of the FIB cross-section revealing solid Cu−Ni nanowires (dark) embedded in the alumina template (light). Energy-filtered transmission electron microscopy (EFTEM) utilizing the electron energy-loss spectrum (EELS) was used to produce images showing the compositional variation. Figure 4b is an EFTEM ratio image[27,28] formed using the Ni $L_{3,2}$ absorption edge at ~855 eV energy loss and showing higher nickel content around the perimeter of the nanowires. Representative energy dispersive, X-ray spectra (EDS) of the core and shell regions are shown in Figure 4d,e. For this analytical work, we prepared samples on Mo TEM grids to avoid spurious X-rays from the usual Cu grids. EDS spectra were collected with

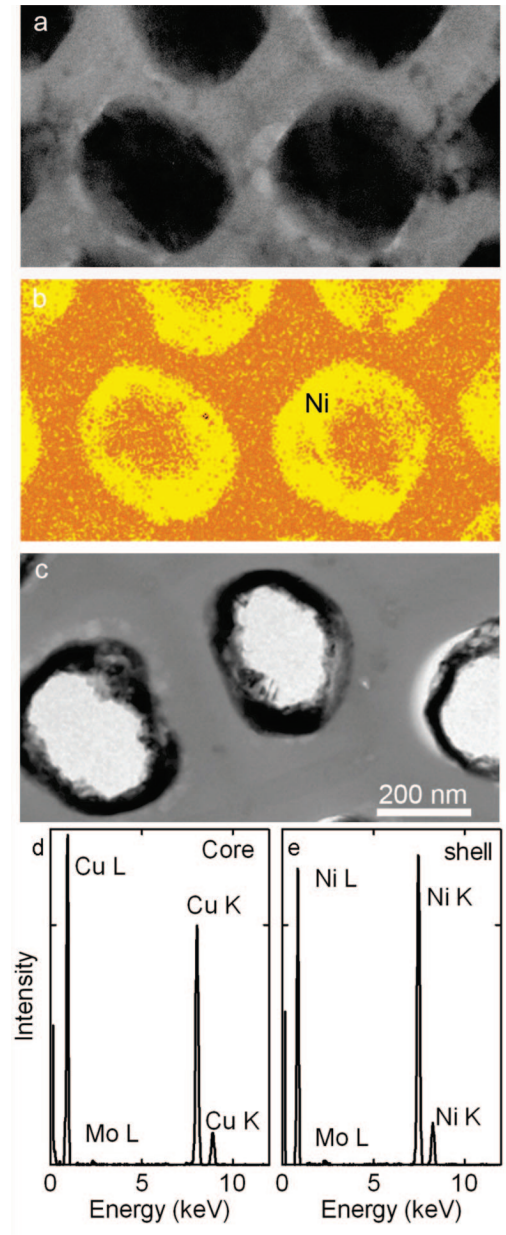

Figure 4. (a) TEM cross-section image of the Cu−Ni core/shell nanowires in the alumina template, (b) corresponding EFTEM image with core/shell structure, (c) TEM cross-section image of Ni nanotubes after etching the Cu-rich core, (d) EDS spectrum of the Cu-rich core in as-deposited Cu−Ni nanowires, and (e) EDS spectrum of the Ni-rich shell in Cu−Ni nanowires after etching.

2−5 nm spot sizes using an Oxford INCA 6367 Si(Li) detector with Oxford INCAx-stream digital pulse height analyzer. Samples were mounted in a Be-cup, low background Gatan holder tilted to 20° to provide nominal takeoff angles of 40°. For quantification, X-ray background was removed by subtracting a third-order, multipolynomial modeled background fit in seven energy windows from 0.17 to 7.72 keV wide. Cu−K and Ni−K peaks were fit to Gaussians and reduced with ZAF (backscatter/absorption/fluorescence) correction using EMISPEC ESVision 4.0 software. Since the samples are binary, resulting compositional ratios were normalized to 100% and showed that the shells are $Ni_{0.994}Cu_{0.006}$ while cores are $Ni_{0.006}Cu_{0.994}$. Typical errors on

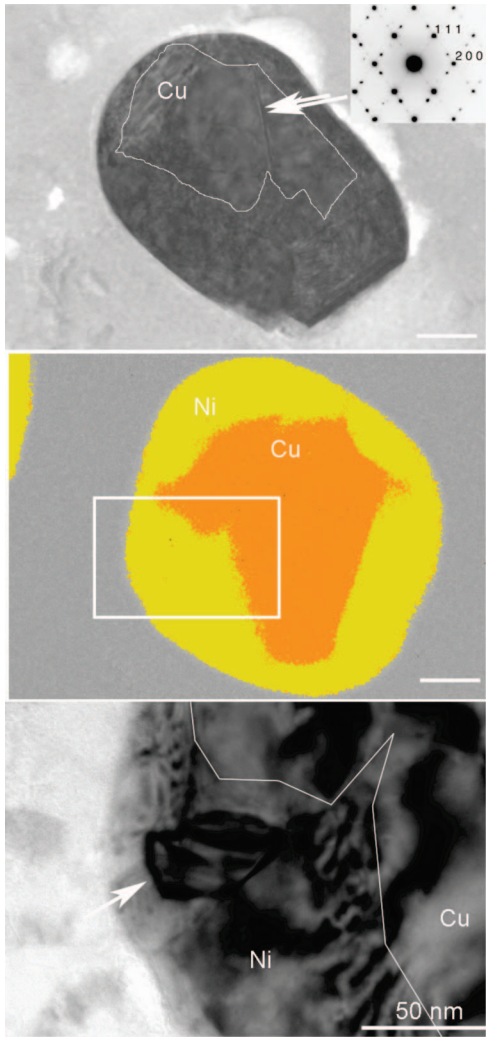

Figure 5. (a) TEM cross-section image of a Cu−Ni nanowire with the Cu-rich core outlined. The inset shows a [022] zone-axis, selected-area electron diffraction pattern showing twinning (arrowed) in the Cu core. (b) EFTEM jump-ratio image of a Cu-rich core in a Cu−Ni nanowire showing phase separation. (c) Bright-Field TEM image of the region indicated in panel b. Note that the sample is in a different orientation than in panel b, so the perspective has changed. In this orientation, one of the discrete, small Ni grains is visible (arrowed). The approximate position of the Ni−Cu phase boundary is traced by the white line but partially obscured by diffraction contrast.

such TEM EDS analyses are approximately ±0.3%. Gallium was below the detection limit in all EDS spectra, highlighting that ion beam damage from FIB milling is negligible. Clearly, the nanowires have almost pure Cu cores with almost pure Ni shells. After etching the copper-rich phase, FIB preparation allows TEM imaging of the remaining nickel-rich nanotubes (Figure 4c).

Figure 5 shows a cross-sectional bright-field TEM image of Cu−Ni core/shell nanowires. The strong diffraction contrast and small grain size of the shells prevent visualization of the complete grain structure of the wires in a single micrograph. There is evidence, however, that in general the Cu-rich core is composed of one or just a few large Cu grains while the surrounding Ni-rich shell is characterized by a large number of smaller grains. Figure 5a shows an example of a large copper grain, about 100 nm in size, bisected by a twin boundary (arrowed). The inset in Figure 5a is a selected-area electron diffraction (SAED) pattern showing the extra spots due to twinning on (111) planes. The EFTEM ratio image map in Figure 5b shows a typical, irregularly shaped Cu-rich core. The higher magnification TEM image in Figure 5c shows that the boundary between the core and shell is usually obscured by diffraction contrast, possibly due to growth strain at the interface.[29,30] Figure 5c also shows an approximately 25 × 50 nm grain of Ni. Tilting in the TEM reveals many such grains in the shells. Indeed, SAED shows that the shells have discontinuous ring patterns consistent with a fine, polycrystalline structure. These results suggest that the deposition process involves the growth of large copper grains surrounded by much smaller nickel islands.

The results presented here demonstrate that our template based electrodeposition method can make Cu−Ni nanowires with nearly pure Cu cores and Ni shells. The FIB lift-out technique is a powerful tool facilitating production of TEM samples perpendicular to the nanowire axis. Such samples allow TEM-based studies to investigate variables such as composition and grain structure which are critical to understand structure−property relationships in nanowire fabrication.

The FIB-TEM method not only provides a technique to characterize nanowires and nanotubes fabricated by template synthesis but also provides the possibility to characterize free-standing nanowires and nanotubes fabricated by other methods, such as CVD and PVD. In the latter case, a polymer can be used to fill the space between the nanowires or nanotubes, providing the support for FIB preparation. Hence the FIB-TEM method should have broad applicability in the study of a wide range of quasi-one-dimensional structures.

Acknowledgment. This work was supported by the JHU MRSEC (NSF grant number DMR05-20491). D.E. acknowledges support from DOE (DOE BES grant DE-FG02-89ER14074).

References

(1) Chen, M.; Searson, P. C.; Chien, C. L. *J. Appl. Phys.* **2003**, *93* (10), 8253–8255.
(2) Sapp, S. A.; Lakshmi, B. B.; Martin, C. R. *Adv. Mater.* **1999**, *11* (5), 402–404.
(3) Tian, M. L.; Wang, J. U.; Kurtz, J.; Mallouk, T. E.; Chan, M. H. W. *Nano Lett.* **2003**, *3* (7), 919–923.
(4) Whitney, T. M.; Jiang, J. S.; Searson, P. C.; Chien, C. L. *Science* **1993**, *261* (5126), 1316–1319.
(5) Ji, C. X.; Searson, P. C. *J. Phys. Chem. B* **2003**, *107* (19), 4494–4499.
(6) Bao, J.; Tie, C.; Xu, Z.; Zhou, Q.; Shen, D.; Ma, Q. *Adv. Mater.* **2001**, *13* (21), 1631–1633.
(7) Escrig, J.; Daub, M.; Landeros, P.; Nielsch, K.; Altbir, D. *Nanotechnology* **2007**, *18* (44), 445706.
(8) Nielsch, K.; Castano, F. J.; Matthias, S.; Lee, W.; Ross, C. A. *Adv. Eng. Mater.* **2005**, *7* (4), 217–221.
(9) Law, M.; Greene, L. E.; Johnson, J. C.; Saykally, R.; Yang, P. D. *Nat. Mater.* **2005**, *4* (6), 455–459.
(10) Phok, S.; Rajaputra, S.; Singh, V. P. *Nanotechnology* **2007**, *18* (47),
(11) Liu, Z.; Searson, P. C. *J. Phys. Chem. B* **2006**, *110* (9), 4318–4322.
(12) Son, S. J.; Reichel, J.; He, B.; Schuchman, M.; Lee, S. B. *J. Am. Chem. Soc.* **2005**, *127* (20), 7316–7317.
(13) Nicewarner-Pena, S. R.; Freeman, R. G.; Reiss, B. D.; He, L.; Pena, D. J.; Walton, I. D.; Cromer, R.; Keating, C. D.; Natan, M. J. *Science* **2001**, *294* (5540), 137–141.

(14) Salem, A. K.; Searson, P. C.; Leong, K. W. *Nat. Mater.* **2003**, *2* (10), 668–671.
(15) Tian, B. Z.; Zheng, X. L.; Kempa, T. J.; Fang, Y.; Yu, N. F.; Yu, G. H.; Huang, J. L.; Lieber, C. M. *Nature* **2007**, *449* (7164), 885–890.
(16) Liu, Z.; Xia, G. Q.; Zhu, F.; Kim, S.; Markovic, N.; Chien, C. L.; Searson, P. C. *J. Appl. Phys.* **2008**, *103* (6).
(17) Giannuzzi, L. A.; Kempshall, B. W.; Schwarz, S. M.; Lomness, J. K.; Prenitzer, B. I.; Stevie, F. A. FIB lift-out specimen preparation techniques. In *Introduction to Focused Ion Beams: Instrumentation, Theory, Techniques and Practice*; Giannuzzi, L. A., Stevie, F. A., Eds.; Springer: New York, 2005; p 358.
(18) Giannuzzi, L. A.; Stevie, F. A. *Micron* **1999**, *30* (3), 197–204.
(19) Phaneuf, M. W. *Micron* **1999**, *30* (3), 277–288.
(20) Forster, H.; Schrefl, T.; Dittrich, R.; Suess, D.; Scholz, W.; Tsiantos, V.; Fidler, J.; Nielsch, K.; Hofmeister, H.; Kronmuller, H.; Fischer, S. *IEEE Trans. Magn.* **2002**, *38* (5), 2580–2582.
(21) ASM International. *Binary alloy phase diagrams*; ASM International: Materials Park, OH, 1996.
(22) Wang, C. P.; Liu, X. J.; Jiang, M.; Ohnuma, I.; Kainuma, R.; Ishida, K. *J. Phys. Chem. Solids* **2005**, *66* (2−4), 256–260.
(23) Menezes, S.; Anderson, D. P. *J. Electrochem. Soc.* **1990**, *137* (2), 440–444.
(24) Sun, L.; Chien, C. L.; Searson, P. C. *Chem. Mater.* **2004**, *16* (16), 3125–3129.
(25) Kiener, D.; Motz, C.; Rester, M.; Jenko, M.; Dehm, G. *Mater. Sci. Eng. A* **2007**, *459* (1−2), 262–272.
(26) Newbury, D. *J. Res. Natl. Inst. Stand. Technol.* **2002**, *107* (6), 605–619.
(27) Egerton, R. F. *Electron Energy-Loss Spectroscopy in the Electron Microscope*, 2nd ed.; Plenum: New York, 1996; p 485.
(28) Fultz, B.; Howe, J. M. *Transmission Electron Microscopy and Diffractometry of Materials*, 2nd ed.; Springer-Verlag: Heidelberg, 2002; p 748.
(29) Moffat, T. P. *J. Electrochem. Soc.* **1995**, *142* (11), 3767–3770.
(30) Hirsch, P. B.; Howie, A.; Nicholson, R. B.; Pashley, D.; Whelan, M. J. **1966**, 563.

NL080492U